Tunnelling and Underground Space Technology 108 (2021) 103692

Contents lists available at ScienceDirect

Tunnelling and Underground Space Technology incorporating Trenchless Technology Research

journal homepage: www.elsevier.com/locate/tust

Single-channel blowing-in longitudinal ventilation method and its application in the road tunnel

Chao Guo [a,b], Zhiyuan Li [c], Hehua Zhu [a,b], Li Zhao [b], Zhiguo Yan [a,b,*]

[a] State Key Laboratory of Disaster Reduction in Civil Engineering, Tongji University, Shanghai 200092, China
[b] Department of Geotechnical Engineering, Tongji University, Shanghai 200092, China
[c] Department of Civil Engineering, Stanford University, CA 94305, USA

ARTICLE INFO

Keywords:
Road tunnel
Longitudinal ventilation
Single channel
Energy consumption

ABSTRACT

The longitudinal ventilation method is widely used in extra-long tunnels because of its simple ventilation mode and lower construction and operation costs. This paper originally proposes a new longitudinal ventilation method, the single-channel blowing-in longitudinal method. Only one ventilation channel is set between uphill line and downhill line of main tunnel, and relatively fresh air near the entrance of the downhill line is sent to the section close to the uphill line exit through the ventilation channel. The authors deduced the ventilation theory, design method and applicable conditions in detail, analyzing six cases to reveal the variation regulation of optimal location of single-channel x_{fit}, one-year ventilation energy consumption P_{one}, total ventilation energy consumption P_{total}, and applicable scope of the tunnel length L_{max}. The results suggest the following. (1) The optimal location of single-channel x_{fit} enable the total ventilation energy consumption in serving period P_{total} to be the minimal, but usually it cannot let one-year energy consumption P_{one} reach the minimum. (2) The single-channel system makes full use of the surplus fresh air and the piston effect of traffic wind in the tunnel, showing a better energy-efficient property from a long-term perspective (3) For the whole serving period, x_{fit} and P_{total} is relatively fixed when the traffic volume changes linearly. Meanwhile, this method has been successfully applied to China Mingtang Mountain Tunnel, and the relevant engineering application experience would be helpful for the similar projects.

1. Introduction

The seventies and eighties of the last century witnessed the worldwide mainstream of road tunnel ventilation types varying from horizontal ventilation such as Holland Tunnel (Lesser et al., 1987) in New York city and Frejus Road Tunnel which connects France and Italy and semi-horizontal ventilation, for example, Cross Harbor Tunnel (Chan et al., 1996) in Hong Kong and Er-lang Mountain Tunnel (Liu et al., 2011) in Sichuan, China to longitudinal ventilation, for instance, Shanghai South Hongmei Road Tunnel (Guo et al., 2013) in China and San Bernardino Road Tunnel in Switzerland.

Nowadays, the longitudinal tunnel ventilation systems have been applied in many highway tunnels owing to their lower construction and operation costs and effectiveness of controlling smoke during fire emergencies. The longitudinal ventilation method is widely utilized with the combination of full jet fans and vertical or inclined shafts. By making use of this combination, shafts divide the tunnel into several sections so that the air volume can be controlled flexibly, also the traffic flow provides piston wind which leads to fewer jet fans. This ventilation design has been adopted by lots of traffic constructions, such as Kan-Etsu Tunnel (Asagami and Nagataki, 1988) and Tokyo Bay tunnel in Japan (Yamada and Ota, 1999), as well as Qinling-zhongnan Mountain Tunnel (Yan et al., 2006a, 2006b) in China. The increasing need for longitudinal ventilation stimulates further research on this method. Up till now, for longitudinal ventilation tunnel, many scholars have studied the arrangement of jet fans (Betta et al., 2009, 2010; Pei and Pan, 2014; Costantino et al., 2014), the distribution of pollutant concentration (Wang et al., 2019b), the evacuation and fire smoke (Carvel et al., 2001; Vauquelin and Wu, 2006; Zhang et al., 2019a, 2020, 2021b; Guo et al., 2020) and the structure thermal performance at high temperature (Zhang et al., 2019b, 2021a) from a perspective of theoretical derivation, numerical analysis, model experiments and field experiments.

However, the construction cost of ventilation shafts is relatively high, let alone the operating and maintenance expense of fans in shafts. Considering these disadvantages, some scholars began to study new

* Corresponding author at: State Key Laboratory of Disaster Reduction in Civil Engineering, Tongji University, 1239 Siping Road, Shanghai 200092, China.
E-mail address: yanzguo@tongji.edu.cn (Z. Yan).

https://doi.org/10.1016/j.tust.2020.103692
Received 20 November 2019; Received in revised form 30 May 2020; Accepted 25 October 2020
Available online 13 December 2020
0886-7798/

Nomenclature

A_r	Clearance area of the tunnel (m^2)
A_j	Area of the jet fan (m^2)
$C(x)$	Pollutant concentration of the tunnel cross section x (mg/m^3)
C_0	Pollutant concentration at the tunnel portal (mg/m^3)
D_r	The equivalent diameter of the tunnel cross section (m)
H	The elevation difference between the tunnel portals (m)
k	The wind pressure coefficient
k_l	Motor capacity safety factor
L_i	Tunnel line i or the length of tunnel line L_i (m, $i = 1,2$)
L_{ratio}	Traffic volume Proportion of tunnel uphill line
L_{max}	The applicable scope of tunnel (m)
M_1	Motor input power (kW)
N_i	Designed traffic volume of line L_i (pcu/h, $i = 1,2$)
P_{total}	Total ventilation energy consumption for the serving period (kW)
P_{one}	One-year ventilation energy consumption (kW)
p_{tot}	Axial fan design full air pressure (Pa)
P_1	The ratio of pollutant concentration at joint between Line L_1 and single-channel L_3 to pollutant concentration limit
P_2	The ratio of pollutant concentration at joint between Line L_2 and single-channel L_3 to pollutant concentration limit
Q_{0i}	Required air volume of tunnel line L_i (m^3/s, $i = 1,2$)
Q_i	Designed air volume of a certain section (m^3/s, $i = 1,2,3$)
$Q_{req(co)}$	Required air volume of the CO dilution (m^3/s)
$Q_{req(VI)}$	Required air volume of the smoke dilution (m^3/s)
$Q_{req(ac)}$	Required air volume of the air change (m^3/s)
Q_b	Air volume of axial flow fan (m^3/s)
Q_{3fresh}	the equivalent fresh air content in single-channel(m^3/s)
q	Vehicular source strength ($mg/(s\cdot m^3)$)
S_{kw}	Total input power of axial fan (kW)
S_1	The static pressure at the lower portal of the tunnel (Pa)
S_2	The static pressure at the higher portal of the tunnel (Pa)
u_0	Average wind speed at tunnel portal (m/s)
v_n	Natural wind speed inside the tunnel (m/s)
v_r	Wind speed inside the tunnel (m/s)
v_b	Air velocity in single-channel (m/s)
v_j	Wind speed at the outlet of the jet fan (m/s)
v_w	The ground-surface natural wind velocity outside the tunnel (m/s)
x	The distance between the single-channel and the entrance of Line L_1 (m)
x_{fit}	The optimal location of single-channel (m)
Δp_{ri}	The tunnel ventilation resistance (Pa)
Δp_{ti}	The tunnel traffic wind pressure (Pa)
Δp_{mi}	The tunnel natural wind pressure (Pa)
Δp_i	The boosting capacity of mechanical ventilation (Pa)
Δp_d	Total pressure loss in single-channel (Pa)

Greek symbols

θ	The angle between the single channel and the exit direction of L_1
Δ	The distance between the entrance of the L_1 and the exit of the L_2 (m)
λ	The loss coefficient of the wall frictional resistance
ρ	Air density (kg/m^3)
ρ_{ave}	The average air density at two portals of the tunnel (kg/m^3)
ρ_{in}	The air density in the tunnel (kg/m^3)
ρ_i	The air density near the tunnel portal (kg/m^3)
ξ_{ein}	Local resistance coefficient of at the tunnel entrance
ξ_{eout}	Local resistance coefficient of at the tunnel exit
η	Reduction coefficient of friction loss at the position of the jet fan.
η_m	The motor efficiency
η_f	The full pressure efficiency of the fan.

longitudinal ventilation methods. Berner and Day (1991) first proposed the double-hole complementary ventilation concept, which dilutes the polluted air in uphill tunnel with fresh air in downhill tunnel through an interchange channel. Then Xia et al. (2013, 2014) discussed its calculation methodology and applied it to China Dabie Mountain Tunnel. Three operation modes, including the full-jet longitudinal ventilation, single U-type ventilation and double-U type ventilation are analyzed in detail. Ideally speaking, the ventilation system does not require ventilation wells, thus reducing initial investment and operation costs of tunnels. Wang et al. (2014) further developed the ventilation scheme and applied it in the Qingniling Highway Tunnel, Lianghekou Tunnel, and Jiuling Mountain Tunnel. Chai et al. (Chai et al., 2018) optimized the method for twin-tunnel complementary ventilation design, considering differences in key pollutants in the uphill and downhill tunnels and the energy consumption of the interchange channels.

Economic as Double-Hole Complementary Ventilation is, there is a non-negligible limitation on its application. The research showed that the Double-Hole Complementary Ventilation should be adopted where the ratio of required air volume between left line and right line is greater than 1.5 or the tunnel line slope is within 1.5% and 2.0% (Wang et al., 2015). From the perspective of ventilation, the design and control method of the double-hole complementary longitudinal ventilation system are more complicated. The reasonable location of the two-hole complementary ventilation system requires a lot of trial results (Xia et al., 2013).

The above relevant literature showed that many scientists achieved the goal of saving construction cost of tunnel ventilation and reducing operating expense by proposing innovative ventilation methods such as double-hole complementary ventilation. However, these methods still have some disadvantages. To overcome these shortcomings, this paper proposes a new ventilation approach for extra-long road tunnels, single-channel blowing-in longitudinal ventilation method.

The paper is organized as follows. Section 2 illustrates the analytical model and basic formulas of the calculation methodology. The key parameters such as optimal location of single-channel, traffic volume and traffic volume proportion of uphill line affecting the ventilation energy consumption and applicable scope of the tunnel length are analyzed in Section 3. In addition, Section 3 discusses the field measurement and the theory validation for single channel ventilation method, which is carried out in the Mingtang mountain tunnel, the first tunnel using this ventilation method in China. Afterwards, Section 4 compares the advantages and disadvantages of the longitudinal ventilation methods including the traditional exhaust and blowing shaft ventilation method, double-hole complementary ventilation method and single-channel blowing-in ventilation method and discusses the emergency ventilation scheme and the limitation of single channel ventilation method. Finally, Section 5 summaries the main conclusions gained from this study and provides beneficial suggestions in tunnel ventilation system design.

2. Single-Channel Blowing-in longitudinal method

2.1. Analytical model

As shown in Fig. 1, the right line L_1 is uphill while the left line L_2 is downhill. With the same traffic speed and traffic volume, it is not far to see that the average air pollutant concentration of Line L_1 is higher than

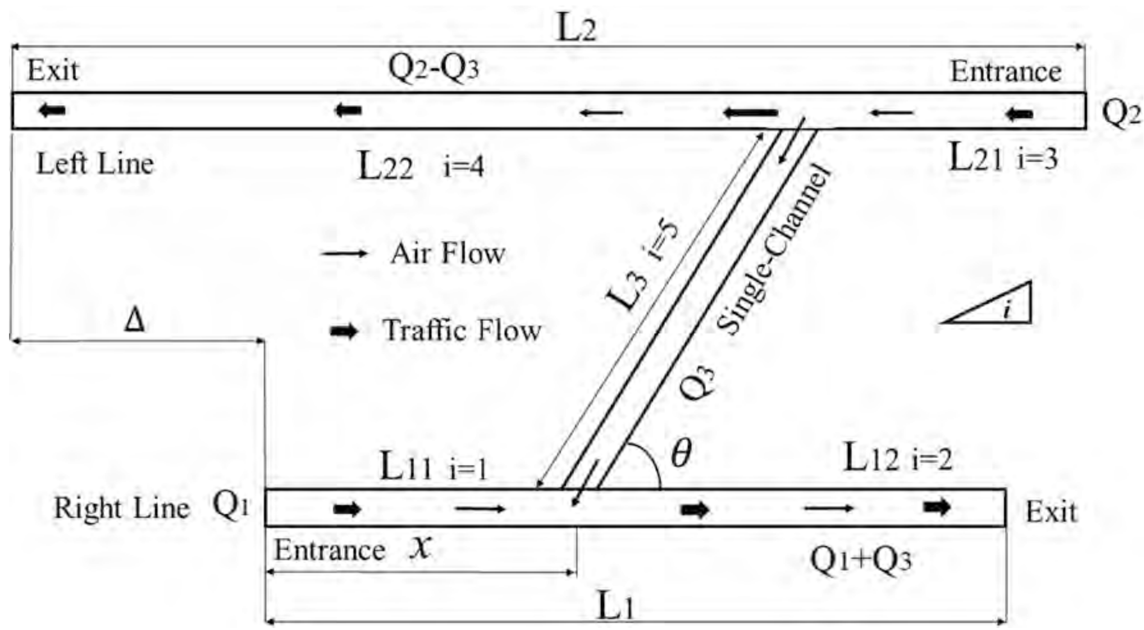

Fig. 1. Diagram of Single-Channel Blowing-in Ventilation Method.

that of Line L_2. The line L_1 requires a large amount of air, which cannot be satisfied by conventional full jet flow ventilation method. On the contrary, the air demand of line L_2 is relatively small and the air volume is rich under operating conditions. The added single-channel L_3 is x m away from the entrance of the right line L_1, and it divided Line L_1 and L_2 into channel L_{11}, channel L_{12}, channel L_{21} and channel L_{22}.

Many scholars have studied the concentration distribution of pollutants in tunnels. For longitudinal ventilation tunnels, the pollutant concentration distribution is shown in Eq. (1), satisfying linear growth (Chang and Rudy, 1990).

$$C(x) = C_0 + \frac{qx}{u_0} \tag{1}$$

In single-channel blowing-in longitudinal method, as shown in Fig. 2, the curves ABCD and EFG indicate the air pollutant concentration distribution of the right tunnel L_1 and the left tunnel L_2 theoretically. After single-channel L_3 is applied, the downward Line L_2 near the entrance transports a part of air into tunnel L_1 near the exit, therefore the pollutant concentration of channel L_{12} decreases rapidly. By selecting a reasonable single-channel position, the pollutant density of both lines can meet the ventilation requirements.

The principle of the single channel is that the "fresh air" near the entrance of the L_2 is sent to the section close to the exit of the L_1 through the ventilation channel. We define P_1 and P_2 as the ratio of pollutant concentration at the joint between line L_1 and single-channel L_3 and the joint between line L_2 and single-channel L_3 to pollutant concentration limit. When the location of the single channel is close to the portal of L_2, $P_2$is less than P_1. The input of "fresh air" through the single channel

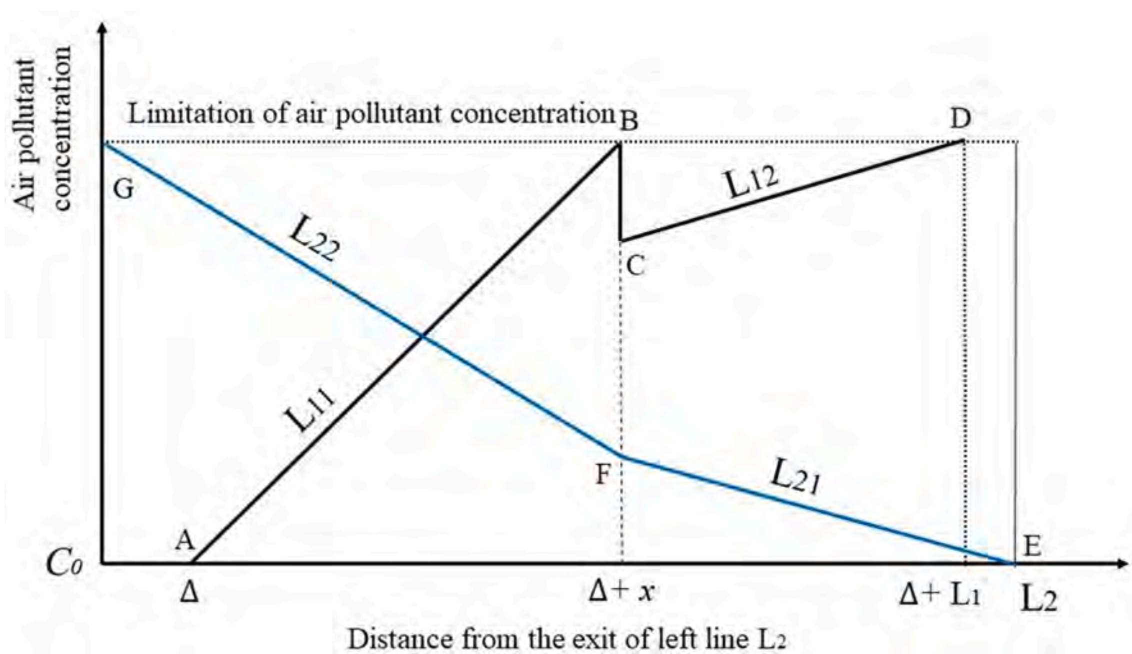

Fig. 2. Pollutant concentration distribution diagram of Single-Channel Blowing-in Ventilation Method.

could reduce the pollutants concentration in channel L_{12}. This is why the curve from point B to point C drops rapidly in Fig. 2.

2.2. Calculation method of Single-Channel ventilation method

2.2.1. Governing equation

In the calculation, there are three criteria according to the Road Tunnels: Vehicle Emissions and Air Demand for Ventilation (PIARC, 2012). Each criterion is considered under different traffic speeds which vary from 10 km/h to 80 km/h. The required air volume Q_{0i} should be the maximum of the CO dilution $Q_{req(co)}$, smoke dilution $Q_{req(VI)}$, and minimum air exchange air volume, as shown in Eqs. (2) and (3).

$$Q_{01} = max\{Q_{1req(VI)}, Q_{1req(CO)}, Q_{1req(ac)}\} \tag{2}$$

$$Q_{02} = max\{Q_{2req(VI)}, Q_{2req(CO)}, Q_{2req(ac)}\} \tag{3}$$

Judging from the features of airflow, the critical sections are (1) the exit of line L_1 (2) the exit of Line L_2 (3) the joint between Line L_1 and single-channel L_3. Note that, Eq. (4), Eq. (5) and Eq. (6) respectively indicates that the concentrations of pollutants at the exit of the Line L_1, the exit of Line L_2, and the joint between Line L_1 and single-channel L_3 exactly reach the air pollutant concentration.

$$Q_{01}\cdot L_2 + Q_{02}\cdot(L_2 - x - \Delta - L_3 cos\theta)\cdot\frac{Q_3}{Q_2} = (Q_1 + Q_3)\cdot L_2 \tag{4}$$

$$Q_{02}\cdot L_2 - Q_{02}\cdot(L_2 - x - \Delta - L_3 cos\theta)\cdot\frac{Q_3}{Q_2} = (Q_2 - Q_3)\cdot L_2 \tag{5}$$

$$Q_{01}\cdot x = Q_1\cdot L_1 \tag{6}$$

As shown in Fig. 3, the curve AC in blue shows the pollutants concentration distribution of the line L_2 under the condition of the required air volume of Q_{02} with the longitudinal ventilation. And the curve ABC in red shows the pollutants concentration distribution of the line L_2 under the condition of the designed air volume of Q_2 when the single-channel blowing-in longitudinal method is used. Next, the derivation principle of Eq. (4) to Eq. (5) will be described in detail.

According to the curve similarity relation in Fig. 3 and Eq. (1), P_2can be calculated from Eq. (7). Then we can derive the equivalent fresh air content in single-channel Q_{3fresh} and designed air volume of Q_2, as shown in Eq. (8) and Eq. (9). Then, the Eq. (5) can be derived from Eq. (7) to Eq. (9).

$$P_2 = \frac{C_3}{C_1} = \frac{L_2 - x - \Delta - L_3 cos\theta}{L_2}\cdot\frac{Q_{02}}{Q_2} \tag{7}$$

$$Q_{3fresh} = (1 - P_2)\cdot Q_3 \tag{8}$$

$$Q_2 = Q_{02} + Q_{3fresh} \tag{9}$$

Similarly, the curve DG in blue and the curve DEFG in red in Fig. 4 show the pollutants concentration distribution of the line L_1 under the condition of the required air volume of Q_{01} with the longitudinal ventilation and the condition of the designed air volume of Q_1 with the single-channel blowing-in longitudinal method. In the same way, we can derive the Eq. (10) and Eq. (11), which are Eq. (4) and Eq. (6).

$$Q_3 = \frac{Q_1\cdot(L_1 - x)}{x\cdot(1 - P_2)} \tag{10}$$

$$Q_1 = \frac{x}{L_1}\cdot Q_{01} \tag{11}$$

2.2.2. Optimal location of the single-channel in one year

In tunnel ventilation calculations, the air can be regarded as an incompressible fluid, and the air flow in tunnel can be regarded as a steady flow. For a one-way traffic tunnel, the traffic wind pressure ΔP_{ti} is shown in Eq. (12). The tunnel ventilation resistance ΔP_{ri} consist of the frictional energy losses $\Delta P_{\lambda i}$ and the local energy losses $\Delta P_{\xi i}$ is shown in Eq. (13). The relationship between natural ventilation pressure ΔP_{mi} and equivalent natural wind velocity v_n in the tunnel is represented as Eq. (14) (Ministry of Communications of PRC, 2014).

$$\Delta P_{ti} = \frac{A_m}{A_r}\cdot\frac{\rho}{2}\cdot\frac{N_j\cdot L_i}{3600\cdot v_t}\cdot(v_t - v_r)^2 \tag{12}$$

$$\Delta P_{ri} = \Delta P_{\lambda i} + \Delta P_{\xi i} = (\lambda\cdot\frac{L_i}{D_r})\cdot\frac{\rho}{2}\cdot v_r^2 + \xi_i\cdot\frac{\rho}{2}\cdot v_r^2 \tag{13}$$

$$\Delta P_{mi} = (\xi_{ein} + \xi_{eout} + \lambda\cdot\frac{L_i}{D_r})\cdot\frac{\rho}{2}\cdot v_n^2 \tag{14}$$

When the wind velocity inside the tunnel affected by natural wind

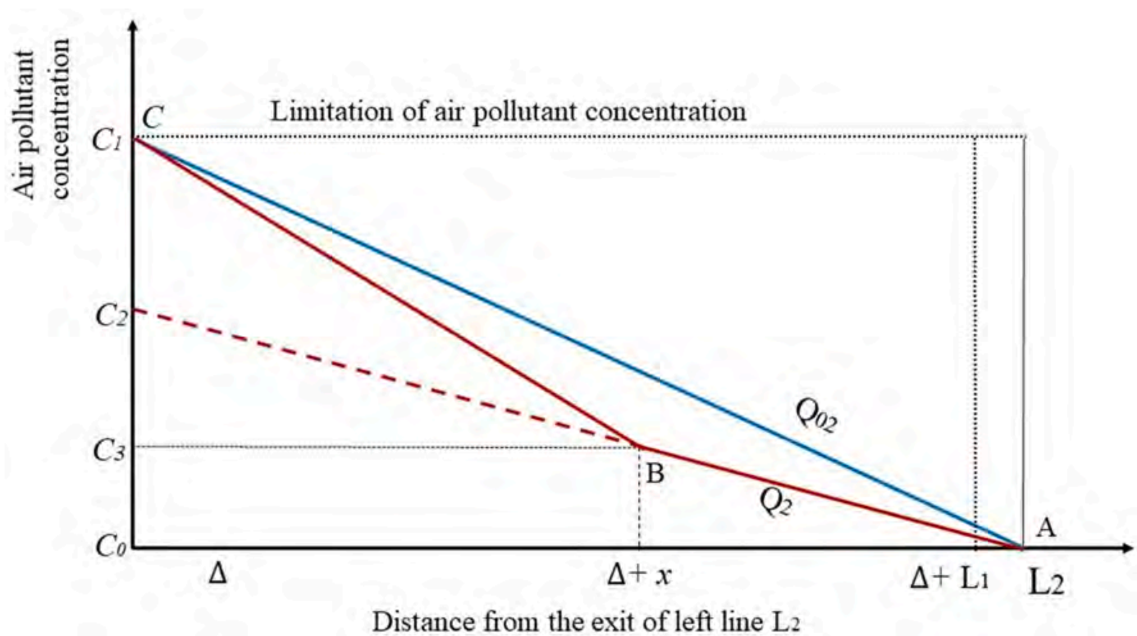

Fig. 3. Pollutant concentration distribution diagram of left line L_2.

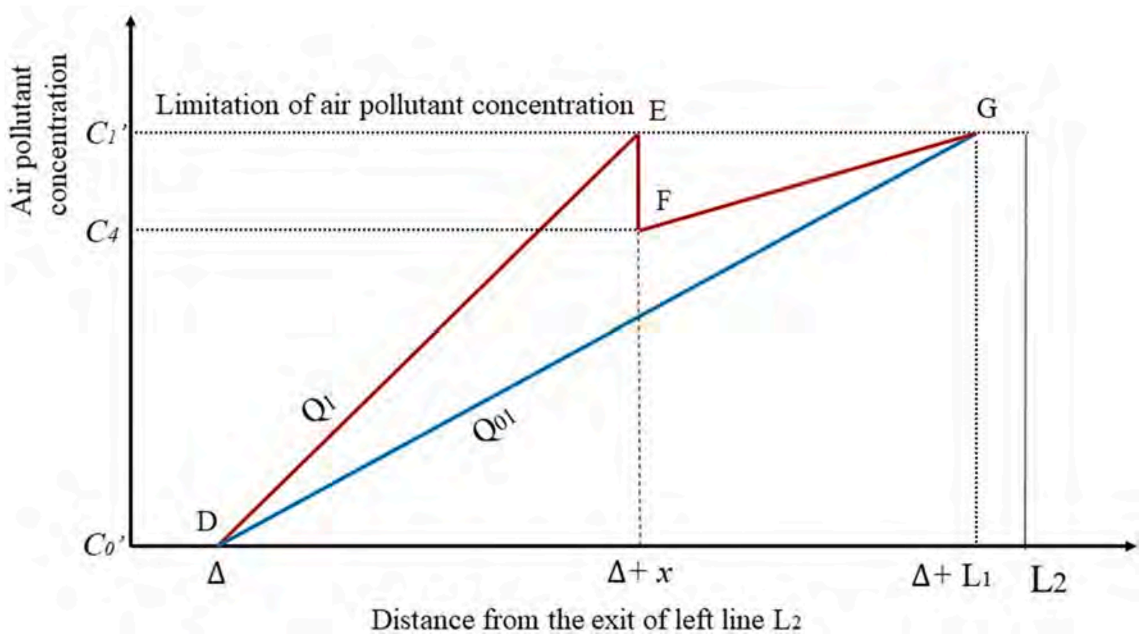

Fig. 4. Pollutant concentration distribution diagram of right line L_1.

outside is in the same direction as the tunnel ventilation, it is regarded as the driving force and the opposite direction as the resistance. But the traditional ventilation design always takes natural wind as resistance force to ensure that the ventilation system can function well, which is a conservative view. Actually, the natural ventilation pressure calculated by Eq. (14) is based on the most unfavorable condition, ignoring the use of natural draught in real operation. It is reasonable and feasible for short and shallow tunnels in the same climatic environment. But for extra-long and deep-buried tunnels located in climate separation zone, notable differences will emerge (Guo et al., 2016; Wang et al., 2019a).

In recent years, some experts studied the natural ventilation calculation method, and carried out a lot of field ventilation measurement analysis. The research results have already been applied to the optimal design of extra-long highway tunnel ventilation systems for energy saving, such as the Liupanshan Tunnel. The natural wind pressure is affected by three main factors: (1) ultra-static pressure difference between entrance and exit caused by horizontal pressure gradient; (2) thermal difference caused by the difference between temperature inside and outside the tunnel; (3) wind wall pressure difference when wind blowing to portals, respectively, as follows (Guo et al., 2016):

$$\Delta P_u = S_1 - S_2 - \rho_{in} g H \tag{15}$$

$$\Delta P_T = (\rho_{ave} - \rho_{in}) g H \tag{16}$$

$$\Delta P_w = k \rho_i v_w^2 / 2 \tag{17}$$

Natural wind force plays an important role in single-channel ventilation, especially in large slope tunnels without shafts. It is of great importance to determine the direction and design velocity of natural wind inside tunnels first for energy saving in the operation of tunnel ventilation. Such issues as geography and climate data need to be fully considered to accurately measure the impact of external wind and natural draught.

When the meteorological data of tunnel, such as temperature, natural wind velocity outside the tunnel, etc., can be obtained through field measurements, the total natural wind pressure ΔP_{mi} can be calculated accurately according to the Eq. (18).

$$\Delta P_{mi} = \Delta P_u - \Delta P_T - \Delta P_w \tag{18}$$

Therefore, the boosting capacity of mechanical ventilation ΔP_i can be obtained based on energy conservation for the entire tunnel is shown in Eq. (19). The energy consumption of the ventilation system in a specific year can be expressed in Eq. (20).

$$\sum_{i=1}^{n} \Delta P_i = \sum_{i=1}^{n} (\Delta P_{ti} - \Delta P_{mi} - \Delta P_{ri}) \tag{19}$$

$$P_{one} = \sum_{i=1}^{n} \Delta P_i \cdot Q_i \tag{20}$$

By solving formulas from Eq. (12) to Eq. (20), the annual energy consumption P_{one} can be expressed as the function of x, the location of the single-channel. The annually minimal energy consumption can be attained if its partial derivative is zero.

$$\frac{\partial P_{one}}{\partial x} = 0 \tag{21}$$

In this regard, the position of the added single-tunnel, x is worked out. Also, the annual ventilation energy consumption can be calculated.

2.2.3. Optimal location of the single-channel in the serving period

In fact, traffic volume changes annually, so the optimal location of single-channel will vary every year. As Eq. (22) shows, P_{total} refers to the overall ventilation energy consumption for T years. As shown in Eq. (23), x_{fit} means the optimal location of single-channel which enables P_{total} to be minimal.

$$P_{total} = \sum_{1}^{T} P_{one}(x) \tag{22}$$

$$min(P_{total}) = \sum_{1}^{T} P_{one}(x_{fit}) \tag{23}$$

3. Engineering application in China Mingtang Mountain tunnel

3.1. Engineering background

China Mingtang Mountain tunnel, which locates at the Yuexi-Wuhan Highway, adopts two-hole One-way traffic design as shown in Fig. 5. The engineering parameters and resistance coefficient of the tunnel are

Fig. 5. China Anhui Mingtang Mountain Tunnel.

shown in Table 1.The frictional resistance coefficients were taken as 0.02. The local resistance coefficients varied according to the tunnel geometry and airflow directions. The local resistance coefficients of tunnel portal and exit are 0.5 and 1, respectively (Ministry of Communications of PRC, 2014; Zhou et al., 2019).

3.2. Feature analysis

This section probes for the variation regulation of optimal location of single-channel x_{fit}, one-year ventilation energy consumption P_{one}, total ventilation energy consumption P_{total}, and applicable scope of the tunnel length $L_{\max}$. According to documents of China Mingtang Mountain Tunnel, the serving period is from 2015 to 2045, thus P_{total} is the sum of ventilation energy consumption for 30 years. Noted the term, "moving right', denotes that the distance x aggrandizes, while 'moving right' means x dwindles. Due to the lack of long-term meteorological data of the Mingtang mountain tunnel, in order to simplify the model calculation, the calculation of natural ventilation pressure adopts Eq. (14) in the theoretical feature analysis. The natural wind speed is regarded as 2.5 m/s and the direction is opposite to the traffic direction according to the Guidelines for Design of Ventilation of Highway Tunnels (Ministry of Communications of PRC, 2014).

3.2.1. Variation regulations of P_{total}-x curves

Example 1: to make data more different under various cases, the ratio of traffic volume of Line L_1 to that of Line L_2 is 7:3 ($L_{\text{ratio}} = 0.7$). It is assumed the traffic volume N has two variation regulations from the year 2015 to 2045: (1) a linearly increasing array from 300 pcu/h to 1500 pcu/h (2) an abruptly increasing array which is 300 pcu/h in 2015–2029 and 1500 pcu/h in 2030–2045.

Table 1
The parameters of energy consumption in Mingtang Mountain Tunnel.

Calculated Parameters	Value	Calculated Parameters	Value
Right Line Length L_1/(m)	7531	Single-channel Area A_3/(m^2)	9.13
Right Line Length L_2/(m)	7548	Blowing shaft length L_4/(m)	340
Clearance area of tunnel A_r/(m^2)	65.18	Blowing shaft area A_4/(m^2)	11.59
Tunnel Equivalent Diameter D_r/(m)	8.29	Exhaust shaft length L_5/(m)	340
Tunnel drag coefficient λ	0.02	Exhaust shaft area A_5/(m^2)	18.62
Local resistance coefficient of tunnel portal ξ_1	0.5	Traffic Volume in Short Term N_1/(pcu/h)	962
Local resistance coefficient of tunnel exit ξ_2	1	Traffic Volume in Long Term N_2/(pcu/h)	1594
Bifurcation Loss Coefficient ξ_1	0.24	Tunnel gradient i/(%)	0.8
Confluence Loss Coefficient ξ_2	0.7	Design speed of automobile v_t/(km/h)	80
Air density ρ/(kg/m^3)	1.29	Automobile Equivalent resistance Area A_m/(m^2)	3
Single-channel length L_3/(m)	55		

According to Fig. 6 and Fig. 7, there are three findings. (1) In all cases, with x increasing and single-channel moving right, P_{total} decreases monotonously then augments strictly. (2) All x_{fit}, corresponding to the location of single-tunnel where the minimal P_{total} is reached, is within 6000 m-7000 m. It can be concluded that the optimal location of the single-channel is relatively stationary where the volume of traffic changes differently. (3) P_{total} varies drastically if x changes a lot, and the maximal P_{total} can be 50 times of minimal P_{total}.

3.2.2. Variation regulations of x_{fit} and P_{one} in one year

Before analyzing cases for serving period, it is necessary to discuss the features of x_{fit}, and P_{one} in a specific year.

Example 2: considering that $L_{\text{ratio}} = 0.3$,0.4,0.5,0.6 and 0.7, also assuming that N is a constant taken from 300 pcu/h to 1500 pcu/h with a step of 100 pcu/h, the N -x_{fit} curves and N - P_{one} curves are presented in Fig. 8 and Fig. 9.

Three regulations are attained. (1) When L_{ratio} is stationary, if x_{fit} increases, single-channel moves right and P_{one} dwindles. Thus, x_{fit} has a negative correlation with P_{one}. (2) When $L_{\text{ratio}} = 0.3$ or $N \leq 800$pcu/h, P_{one} declines with the increasing of N. For other longitudinal ventilation methods, usually energy consumption increases if traffic density ascends. However, because the traffic airflow of the downhill line is fully used, Single-channel Blowing-in Ventilation method can be more energy-efficient even though traffic becomes busier. (3) With the same N, if L_{ratio} descends, the downhill line L_2 takes more traffic flow and P_{one} decreases. This can also be explained that the downhill line provides more fresh air.

3.3. Variation regulations of x_{fit} and P_{total} for the serving period

3.3.1. Case analysis with N being constant for the serving period

Example 3: as same as *Example 2*, $L_{\text{ratio}} = 0.3$,0.4,0.5,0.6, 0.7, and N is a constant taken from 300 pcu/h to 1500 pcu/h with a step of 100 pcu/h.

By analyzing Fig. 10 and Fig. 11, five regulations can be observed. (1) With the same N, if L_{ratio} decreases, P_{total} reduces. This feature is identical with *Example 2*. (2) Different from *Example 2,* there is a positive relationship between x_{fit} and P_{total}. (3) When $L_{\text{ratio}} = 0.3$, 04 or $N \leq$ 900pcu/h, P_{total} declines with the augment of N. Compared with the conditions ($L_{\text{ratio}} = 0.3$ or $N \leq 800$pcu/h) in *Example 2*, the Single-Channel Blowing-in ventilation method shows a better energy-

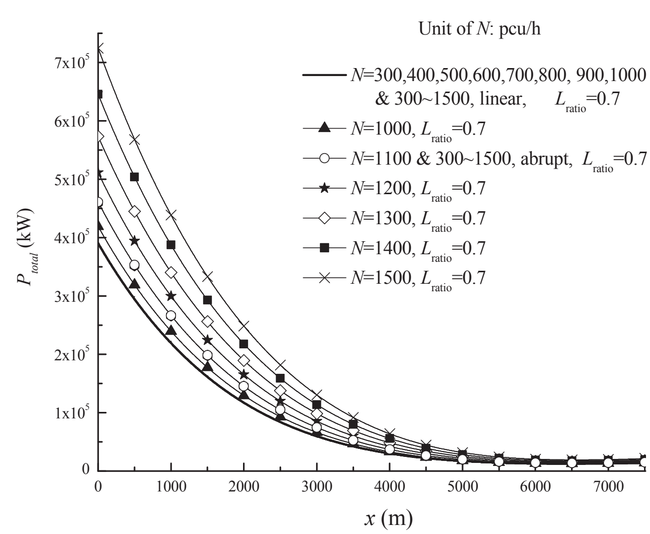

Fig. 6. Position of single-channel x versus total ventilation energy consumption P_{total}.

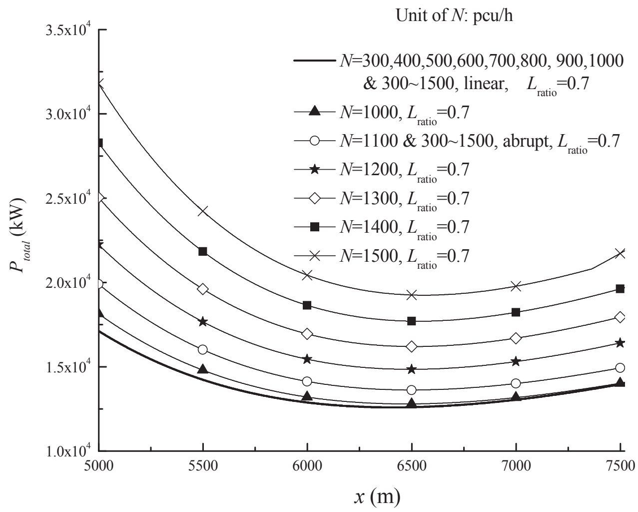

Fig. 7. Position of single-channel x versus total ventilation energy consumption P_{total} (Partly).

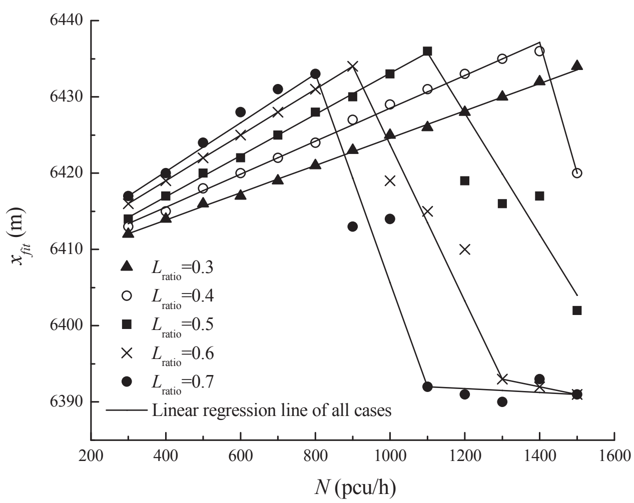

Fig. 8. Designed traffic volume N versus optimal location of single-channel x_{fit}.

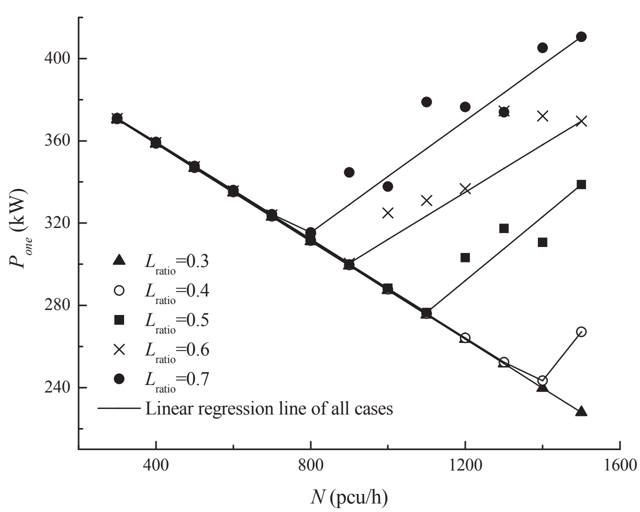

Fig. 9. Designed traffic volume N versus one-year ventilation energy consumption P_{one}.

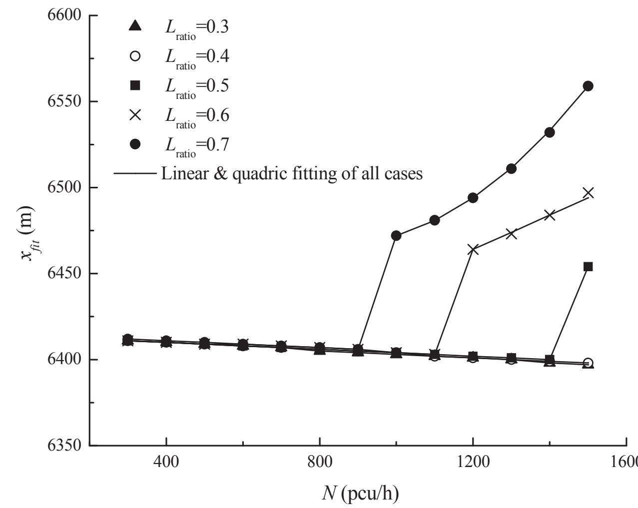

Fig. 10. Designed traffic volume N versus optimal location of single-channel x_{fit}.

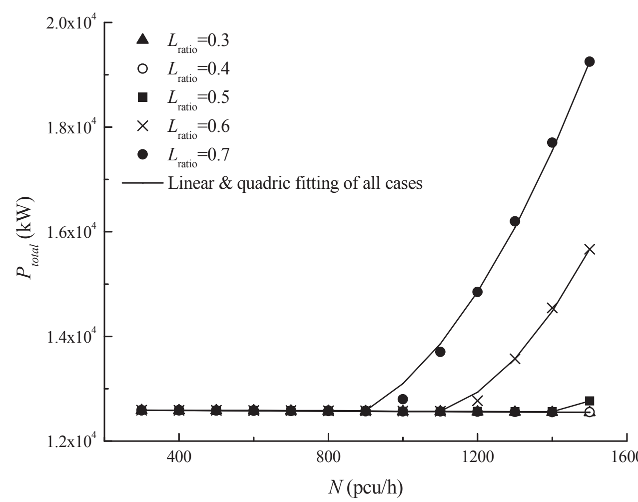

Fig. 11. Designed traffic volume N versus total ventilation energy consumption P_{total}.

efficiency property from a long-term perspective than from a one-year view. (4) By comparing Fig. 6 and Fig. 8, x_{fit} for one year is within 6390 m-6440 m, but x_{fit} for serving period can be as large as 6559 m. Therefore, usually the final design of single-channel cannot make all of P_{one} to reach the minimum, and under some circumstances, none of P_{one} can reach the theoretical minimum. (5) When $L_{\text{ratio}} = 0.3$ or 04, both x_{fit} and P_{total} decreases linearly with the augment of N. However, when $L_{\text{ratio}} \geq 0.5$, x_{fit} and P_{total} shows linear or quadric growth after N reaches a critical value. This feature can be explained by the regulation of the required air volume Q_{01} and Q_{02}. Before N achieves the critical point, the required air volume $Q_{0\text{i}}$ (i = 1,2) is defined by minimal air exchange frequency $Q_{\text{ireq(ac)}}$ which is a constant. If N exceeds the threshold and the uphill line shares a large proportion of traffic, Q_{01} is defined by dust density $Q_{\text{ireq(VI)}}$ which arises sharply when N increases and P_{total} ascends in the same manner.

3.3.2. *Case analysis with N increasing linearly for the serving period*

Actually, designed traffic volume N increases with the year. Taking China Mingtang Mountain Tunnel as an example, $N = 962$pcu/h in the year 2015, and $N = 1594$pcu/h in the year 2034. There are tremendous predicting models for traffic volume (Chen et al., 2016; Sun et al., 2006), and in this paper two fundamental models, linear increasing model and abrupt ascending model are discussed.

Example 4: $L_{\text{ratio}} = 0.3,0.4,0.5,0.6,\ 0.7$, N is linear increasing array with values of 300 pcu/h-900 pcu/h, 600 pcu/h-1200 pcu/h, 900 pcu/h-1500 pcu/h, 300pcu/h-1500 pcu/h.

Fig. 12 and Fig. 13 show regulations of L_{ratio}- x_{fit} curves and L_{ratio}-P_{total} curves, from which three observations can be achieved. (1) With the same N, if L_{ratio} dwindles, P_{total} declines. (2) x_{fit} is positively correlated with P_{total}, which is the same as *Example 3*. (3) Apart from the case where $N = 900$ pcu/h-1500 pcu/h, in other three cases the range of x_{fit} is less than 5 m, and the range of P_{total} is within 13000 kW. This feature denotes that the optimal location of single-channel is relatively fixed if N changes linearly and the average of N is not so huge.

3.3.3. Case analysis with N increasing abruptly for the serving period

Example 5: $L_{\text{ratio}} = 0.3,0.4,0.5,0.6,0.7$, N is abruptly ascending array whose elements are constant from 2015 to 2029, and abruptly change to a larger constant from 2030 to 2045. N = 300 pcu/h-900 pcu/h, 600 pcu/h-1200 pcu/h, 900 pcu/h-1500 pcu/h, 300pcu/h-1500 pcu/h.

As presented in Fig. 14. and Fig. 15., the variation properties can be summarized as followings. (1) With the same N, if L_{ratio} dwindles, P_{total} declines. (2) As same as *Example 3* and *Example 4*, x_{fit} is positively related to P_{total}. (3) Compared with *Example 4*, the stability of x_{fit} and P_{total} becomes worse.

3.3.4. Discussion on applicable scope L_{max}

However, the major constraints of longitudinal ventilation systems are excessive air volume and velocity (Chai et al., 2018). According to Guidelines for Design of Ventilation of Highway Tunnels (Ministry of Communications of PRC, 2014), v_i, the wind speed of channel L_{11}, channel L_{12}, channel L_{21} and channel L_{22}, should be less than 10 m/s, and it can be calculated as Eq. (24) presents.

$$v_i = \frac{Q_i}{A}(i = 1, 2, 3\ or\ 4) \tag{24}$$

Q_1, Q_2, Q_1+Q_3 and Q_2−Q_3 are defined in Eq. (4) to Eq. (6). Then, tunnel maximum wind speed v is introduced in Eq. (25).

$$v = max(v_1, v_2, v_3, v_4) \tag{25}$$

Example 6: $L_{\text{ratio}} = 0.3,0.4,0.5,0.6,0.7$, N is a constant taken from 300 pcu/h to 1500 pcu/h with a step of 100 pcu/h. the lengths of the two tunnel lines are the same value L.

L_{max} is the length of two tunnel lines when v = 10 m/s, and variation

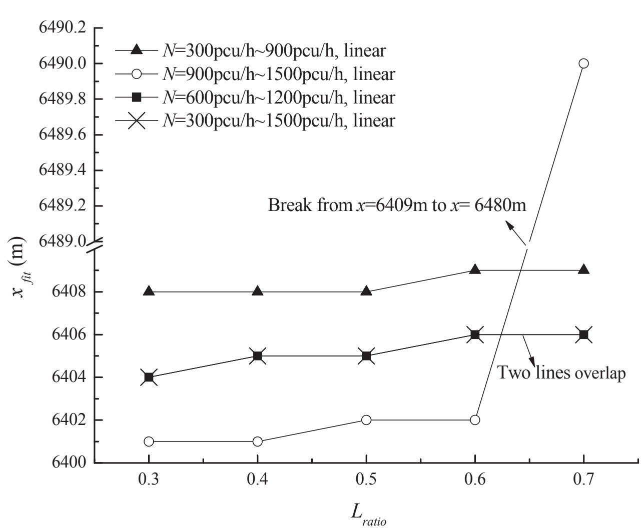

Fig. 12. Traffic volume Proportion of Line L$_1$ L_{ratio} versus optimal location of single-channel x_{fit}.

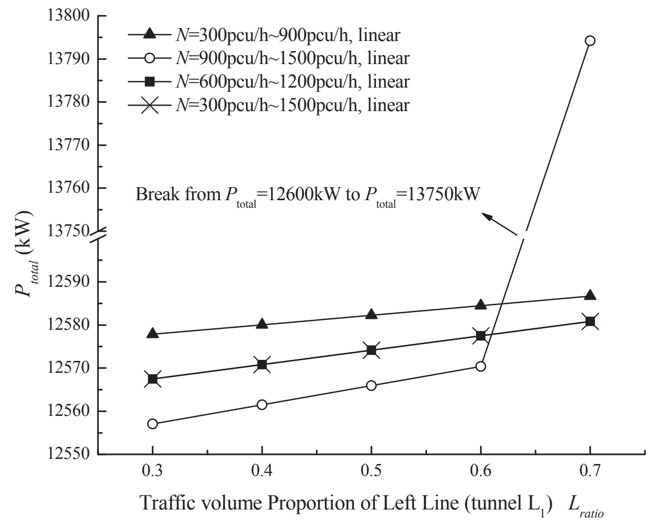

Fig. 13. Traffic volume Proportion of Line L$_1$ L_{ratio} versus total ventilation energy consumption P_{total}.

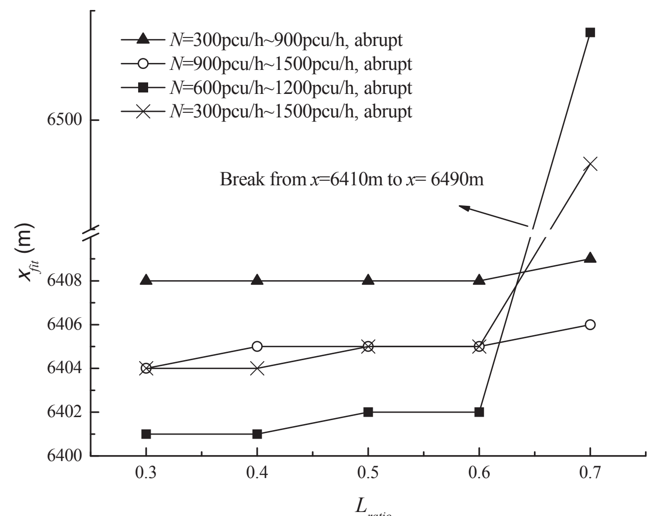

Fig. 14. Traffic volume Proportion of Line L$_1$ L_{ratio} versus optimal location of single-channel x_{fit}.

regulations of v and of applicable scope L_{max} are drawn in Fig. 16 and Fig. 17. Two findings are attained. (1) When $N \leq 600$pcu/h or $L_{\text{ratio}} = 0.3$, v has nothing to do with N or L_{ratio}, and is linear dependent of L. In these cases, $L_{\text{max}} = 12500$ m. (2) With the augment of N and L_{ratio}, v rises while L_{max} descends under most circumstances.

3.4. Design of the single-channel and single-shaft

According to the geological prospecting data, the original design was to install a ventilation shaft at a distance of 4974 m from the entrance of the right line as shown in Fig. 18, and the left line adopts full jet longitudinal ventilation.

Based on the single-channel calculation method with traffic volume N increasing linearly for the serving period, the tunnel ventilation scheme is redesigned, and the single channel ventilation method is adopted. The optimal single channel position is obtained based on different ventilation requirements include the air change and the dilution of pollutants. In the first case, the difference of air volume the uphill tunnel and the downhill tunnel is small, while the difference of the second case is large. In both cases, the optimal single channel position x

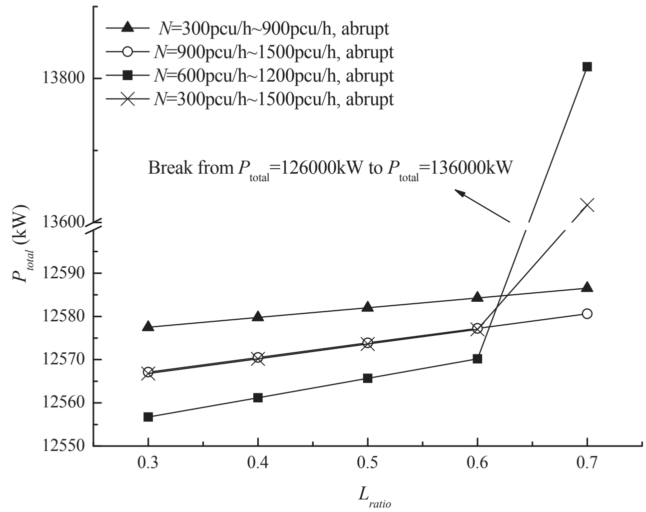

Fig. 15. Traffic volume Proportion of Line L_1 L_{ratio} versus optimal location of single-channel x_{fit}.

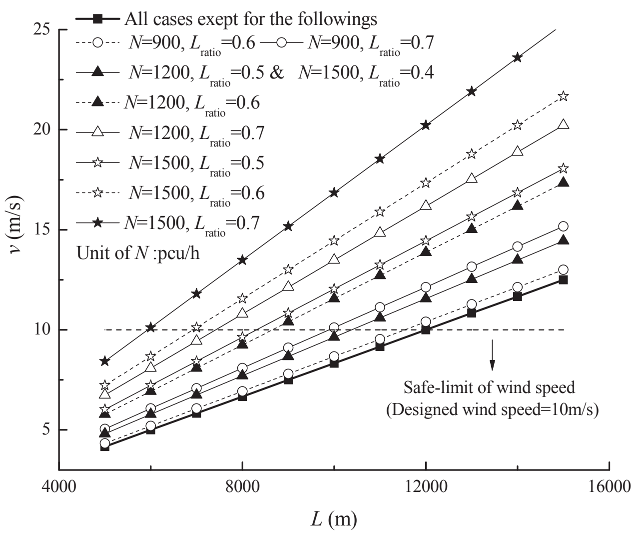

Fig. 16. Tunnel length L vesus designed wind speed of Line L_i v_i.

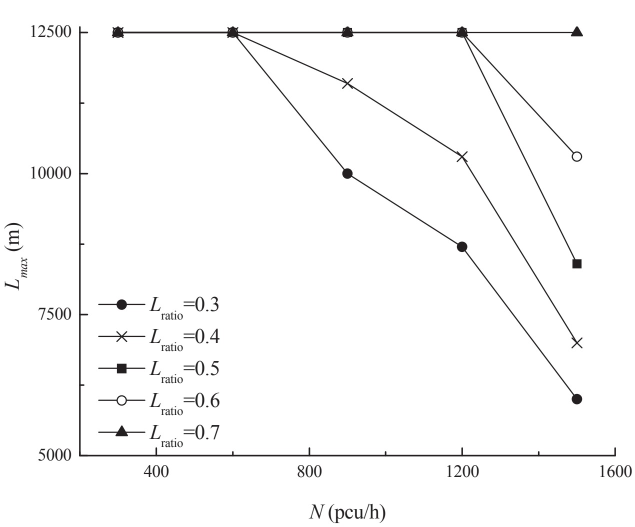

Fig. 17. Designed traffic volume N versus maximal applicable tunnel length $L_{\max}$.

is very close to 5904 m. Taking account of construction convenience, the single-channel ultimately was located at $x = 5813$ m. The specific single-channel method is shown in Fig. 19 and Fig. 20.

3.5. Comparison of energy consumption of the two methods

3.5.1. The theoretical energy consumption

The theoretical energy consumption of traditional shaft ventilation and single channel ventilation are analyzed. The ventilation quantity of Mingtang tunnel is shown in Table 2. In the calculation, the theoretical energy consumption comparison takes into consideration the ventilation resistance of each section ΔP_{ri} and the natural wind pressure ΔP_{mi}, except the traffic wind pressure ΔP_{ti}. The short-term traffic volume and long-term traffic volume are shown in Tables 3–6. And the energy consumption can be reduced by 36.34% in short-term traffic volume compared to the original ventilation design, and 44.82% in long-term traffic volume without considering the effect of traffic wind power.

3.5.2. The theoretical energy consumption equipped with fans

The traffic speed affects the traffic wind pressure ΔP_{ti}, and has a great impact on the number of open jet fans in the tunnel. Therefore, traffic wind power ΔP_{ti} is taken into account when the jet fans and axial fans are arranged at different traffic speeds. According to the tunnel resistance loss in theoretical energy consumption, the actual power of jet fans and axial fans can be calculated. Both the two methods adopted 1120 model jet fan, which can provide lifting pressure as shown in Eq. (26).

$$\Delta p_j = \rho \cdot v_j^2 \cdot \frac{A_j}{A_r} \cdot \left(1 - \frac{v_r}{v_j}\right) \cdot \eta \tag{26}$$

The power of the axial fan can be calculated from the total pressure loss in the single-channel and the blowing and exhaust shafts according to the following Eqs. (27) to (29).

$$p_{\rm tot} = 1.1 \times \left(\frac{\rho}{2} v_{\rm b}^2 + \Delta p_{\rm d}\right) \tag{27}$$

$$S_{\rm kw} = \frac{Q_{\rm b} \cdot p_{\rm tot}}{1000 \cdot \eta_{\rm f}} \tag{28}$$

$$M_1 = \frac{S_{kw}}{\eta_m} \times k_l \tag{29}$$

In the comparative analysis of energy consumption, it is assumed that the ventilation facilities opening time of the two methods are same per day, and the energy saving ratio can be calculated according to the designed fan power. As can be seen from Table 7 and Table 8, the energy saving ratio increases significantly with the vehicle speed growing. In the case of traffic congestion, the energy saving effect of the single-channel method is not obvious. But under normal operation, the energy consumption saving ratio is about 73.74% and 55.84% compared to the original ventilation design at speed of 60 km/h in short term and long term. When the cars speed up to a certain point, the piston effect of traffic wind power could offset the ventilation resistance of the tunnel main lines. The jet fans can be closed, but the axial fan still needs to be opened to meet the requirements of air exchange in the tunnel.

At the speed of 80 km/h, the energy saving ratio has reached 90% in the short and long term. The air supply and exhaust shafts segment the tunnel, effectively reducing the pollutants concentration in the tunnel. And the tunnel wind speed is significantly reduced compared to full-jet longitudinal ventilation and the single-channel ventilation method. However, this advantage has led to the drawback of high energy consumption during the operation period. The piston effect of traffic wind is significant, and the wind speed inside the tunnel is large. The single-channel method makes full use of this feature, and only needs to turn on the axial fan with less power to meet the ventilation requirements. However, the advantages of the shaft ventilation method result in the power of its axial fans being much greater than the single channel

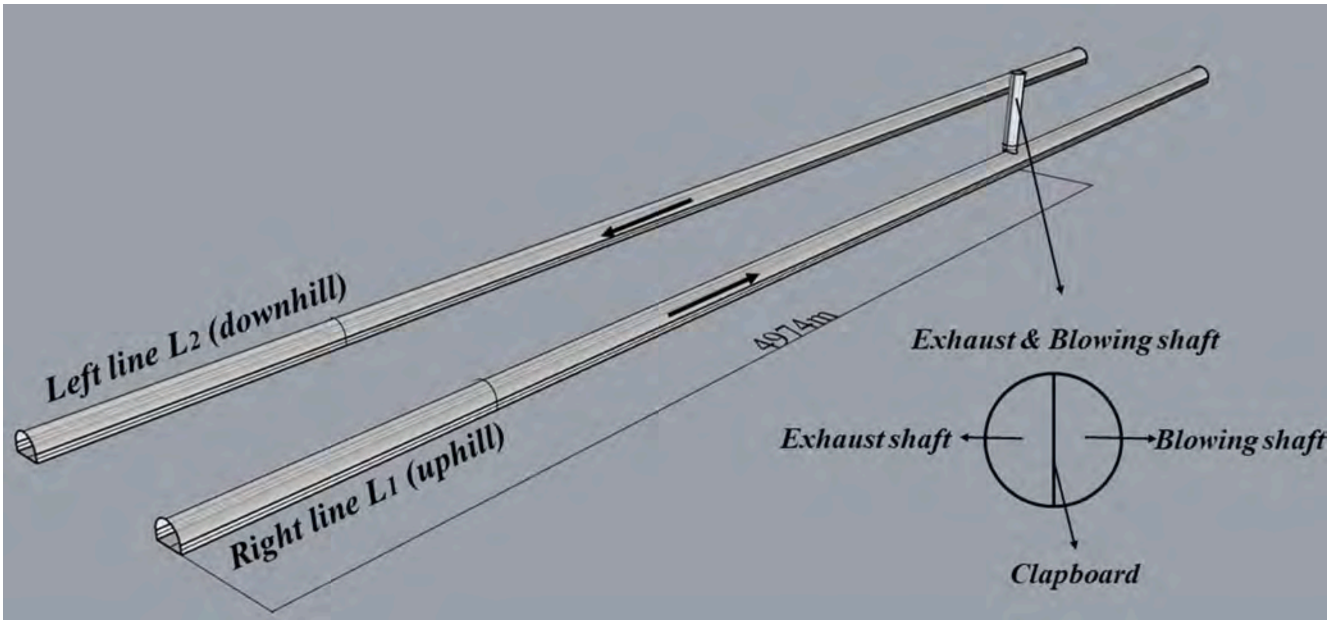

Fig. 18. The original design of single shaft method in Mingtang Mountain Tunnel.

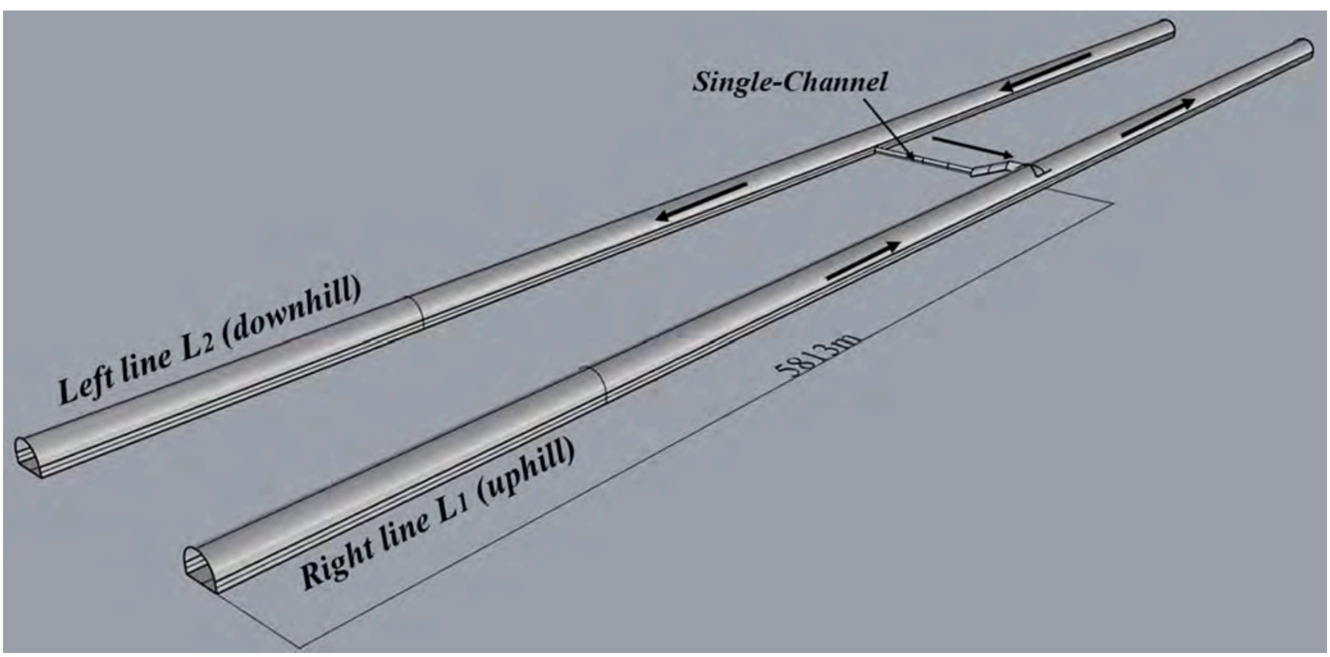

Fig. 19. Design of single-channel method in Mingtang Mountain Tunnel.

method. The arrangement of larger power axial fans in the shaft meets the requirements of air exchange (short term) and dilution of pollutants (long term) respectively.

Overall, the single-channel method has good energy saving effect during the normal operation of the extra-long tunnel. Because it makes full use of the surplus fresh air and the piston effect of traffic wind in the tunnel system. It does not require the conversion of large shafts to outside air, thus greatly reducing the energy consumption during tunnel operation period.

3.6. Field measurement and theory validation

The field ventilation tests were carried out when the Mingtang mountain tunnel was just opened to traffic. As shown in the Fig. 21, four measuring points were arranged at the uphill line L_1 and downhill line L_2 to measure tunnel wind speed. The measuring points M_1, M_2 and M_3 were all placed 20 m away from the single channel, and the measuring point M_4 is 150 m away from the single channel in order to reduce the influence of high-speed jet turbulence on the accuracy of wind speed measurement during the test.

The experimenter stood with his back to the tunnel side wall to measure the wind speed at a height of approximately 2.0 m. A total of 4 testers were arranged for measurements, and each tester was responsible for one measurement point. The air velocity was measured by handheld anemometers (GM8901, 0–45 m/s, ±3%). Fig. 22 shows the test ventilation working condition of the Mingtang Mountain Tunnel. After the wind flow had fully developed, the data was tested in each condition, and the handheld anemometers were read for 10 times during each test

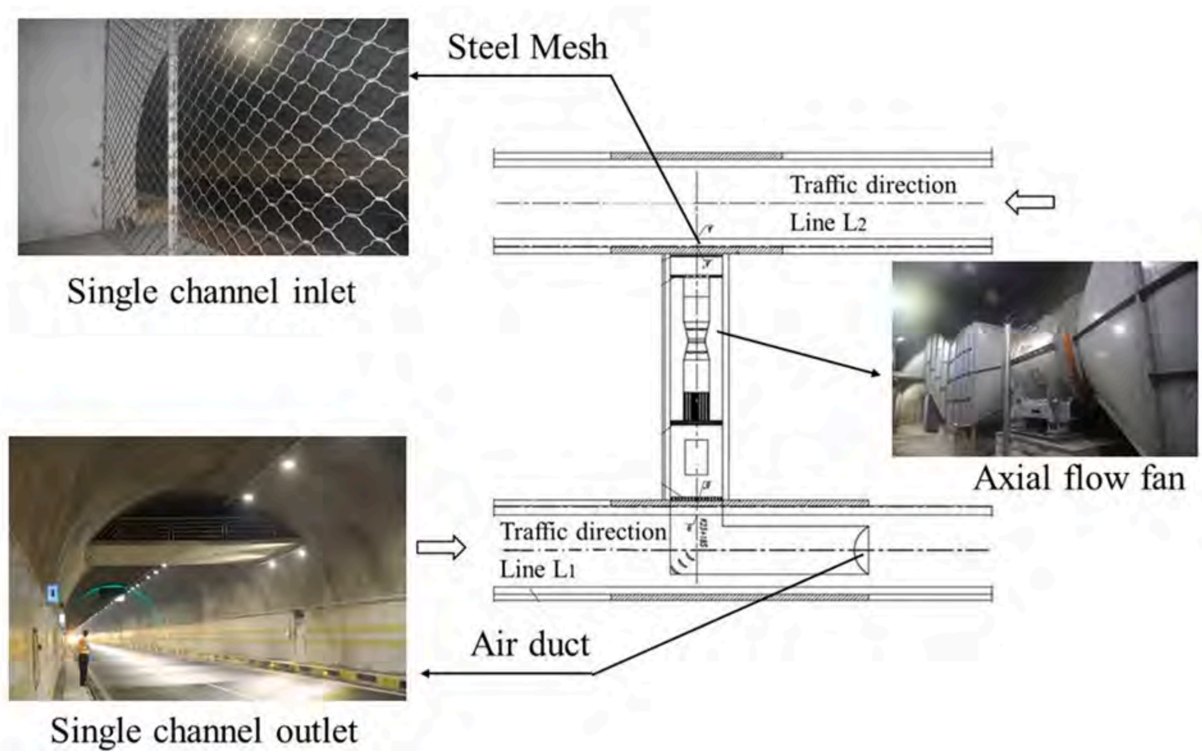

Fig. 20. Diagram of actual lay-out for single-channel method in Mingtang Mountain Tunnel.

Table 2
The ventilation quantity of Mingtang Mountain Tunnel.

Item	Short-term ventilation quantity/(m^3/s)	Long-term ventilation quantity/(m^3/s)
Uphill line L_1	**409.06 (Air exchange $Q_{req(ac)}$)**	409.06 (Air exchange $Q_{req(ac)}$)
	148.83 (Dilution of CO $Q_{req(co)}$)	175.40 (Dilution of CO $Q_{req(co)}$)
	399.10 (Dilution of smoke $Q_{req(VI)}$)	**474.63 (Dilution of smoke $Q_{req(VI)}$)**
Downhill line L_2	**409.98 (Air exchange $Q_{req(ac)}$)**	**409.98 (Air exchange $Q_{req(ac)}$)**
	124.14 (Dilution of CO $Q_{req(co)}$)	146.30 (Dilution of CO $Q_{req(co)}$)
	215.58(Dilution of smoke $Q_{req(VI)}$)	256.37(Dilution of smoke $Q_{req(VI)}$)

Table 3
The theoretical energy consumption of single channel method in short term traffic volume.

Item	Left Line		Right Line		Single-Channel
Tunnel section	L21	L22	L11	L12	L3
Length/(m)	1735	5813	5813	1718	55
Average Air Velocity/(m/s)	7.72	5.96	4.84	6.61	12.57
Air Quantity/(m^3/s)	503.19	388.47	315.47	430.84	114.81
Resistance Loss/(Pa)	209.38	404.79	278.01	188.28	460.1
Energy Consumption/(kW)	105.36	157.25	87.70	81.12	52.82
Total Energy Consumption/(kW)	484.25				

to eliminate the accidental error. The average value of these 10 readings was taken as the test value.

In the field ventilation test, positive denotes that the natural wind direction is the same as the traffic direction, while negative means opposite. The No.3 working condition is the ventilation scheme of the Mingtang mountain tunnel when the traffic speed is approximately 50 km/h with short term traffic volume. Table 9 shows the detailed setup of each experiment and the specific test results

The measured results of No.3 working condition are compared with

Table 4
The theoretical energy consumption of single shaft method in short term traffic volume.

Item	Left Line	Right Line		Shaft	
Tunnel section	L2	L11	L12	Exhaust	Blowing
Length/(m)	7548	4974	2557	340	340
Average Air Velocity/(m/s)	6.29	4.3	2.82	12.90	12.38
Air Quantity/(m^3/s)	409.98	280.27	183.77	240	143.5
Resistance Loss/(Pa)	582.43	203.35	72.11	1139.64	1241.25
Energy Consumption/(kW)	238.78	56.99	13.25	273.51	178.12
Total Energy Consumption/(kW)	760.66				

Table 5
The theoretical energy consumption of single channel method in long term traffic volume.

Item	Left Line		Right Line		Single-Channel
Tunnel section	L21	L22	L11	L12	L3
Length/(m)	1735	5813	5813	1718	55
Average Air Velocity/(m/s)	7.95	5.92	5.62	7.65	14.50
Air Quantity/(m^3/s)	518.18	385.87	366.31	498.63	132.34
Resistance Loss/(Pa)	220.84	400.19	354.44	244.18	460.1
Energy Consumption/(kW)	114.43	154.42	129.83	121.76	60.89
Total Energy Consumption/(kW)	581.33				

Table 6
The theoretical energy consumption of single shaft method in long term traffic volume.

Item	Left Line	Right Line		Shaft	
Tunnel section	L2	L11	L12	Exhaust	Blowing
Length/(m)	7548	4974	2557	340	340
Average Air Velocity/(m/s)	6.29	4.9	3.18	15.05	14.46
Air Quantity/(m^3/s)	409.98	319.38	206.97	280	167.59
Resistance Loss/(Pa)	582.43	248.72	83.07	1550.01	1695.24
Energy Consumption/(kW)	238.78	79.44	17.19	434.00	284.11
Total Energy Consumption/(kW)	1053.52				

the theoretical calculation results as shown in Fig. 23. The maximum and minimum relative errors between the measurement results and the corresponding calculation results are 14.8% and 2.6% for the following reasons. First, the traffic volume was far less than the planning short-term traffic volume at the time of the field ventilation test. Therefore, the traffic wind power due to the piston effect was far less than the designed power. Second, the measuring point M_4 is affected dramatically by the turbulence development of the top air supply, and the error is relatively large.

Basically, the single channel ventilation theoretical calculation method satisfies the requirement of engineering accuracy for tunnel ventilation design. Such issues as geography and climate data need to be fully considered to accurately measure the impact of external wind and natural draught.

4. Discussion

4.1. Comparison with other longitudinal ventilation methods

In recent years, traditional exhaust and blowing shaft ventilation (Yan et al., 2006a, 2006b; Zhang et al., 2018) and new type double-hole complementary ventilation method (Xia et al., 2013; Chai et al., 2018) in longitudinal ventilation have been continuously applied in extra-long tunnels.

The principle of double-hole complementary ventilation is the exchange of air between the uphill tunnel and the downhill tunnel, and the conditions for the ratio of required air volume between uphill line and downhill line is greater than 1.5 or the tunnel line slope is within 1.5% and 2.0% must be met (Wang et al., 2015). From the perspective of ventilation, the design and control method of the double-hole complementary longitudinal ventilation system are more complicated. The reasonable location of the two-hole complementary ventilation system requires a lot of trial results. A section similar to a short duct is formed between the two transverse channels, and the concentration of the pollutants rapidly increases. If the spacing of the transverse channels is too large or the exchange air volume is too large, the pollutants concentration in the short duct may exceed the standard concentration (Xia et al., 2013).

The vertical or inclined shaft ventilation method could effectively eliminate the polluted air in the tunnel and bring fresh air in, which is an effective longitudinal ventilation method, but the civil construction costs and operating costs of axial fans are expensive. When the geological conditions for constructing vertical or inclined shafts are complex, the single-channel method is a good way to replace the vertical or inclined shaft method.

The energy-efficient principle of the single-channel ventilation method is that the tunnel itself (L_{12} and L_{21} in Fig. 1) is used as a “shaft” to send and exhaust air through the link of single-channel. As long as the required air volume of the tunnel is less than the maximum air supply volume of the tunnel, the single-channel ventilation method could be used. It surmounts the limitation that traffic flow of two lines should be distinct. Meanwhile, the single-channel ventilation method simplifies ventilation design and control compared to the double-hole complementary longitudinal ventilation. The power of the single-channel internal axial fans is much smaller than that of the axial-flow fans in the vertical or inclined shafts, which is the main reason for the energy saving of the method.

Table 7
The comparison of theoretical energy consumption equipped with fans in short term traffic volume.

vehicle speed km/h	Single-Channel Method				Single Shaft Method				Energy saving ratio
	Number of jet fans		Axial flow fan power	Total Power/(kW)	Number of jet fans		Axial flow fan power	Total Power/(kW)	
	Left Line	Right Line	Single-channel/(kW)		Left Line	Right Line	Single shaft/(kW)		
30	61	40	145.5	3882.5	54	12	1283	3725	−4.23%
40	47	26	145.5	2846.5	48	6	1283	3281	13.24%
50	22	11	145.5	1366.5	38	0	1283	2689	49.18%
60	9	3	145.5	589.5	26	0	1283	2245	73.74%
70	0	0	145.5	145.5	16	0	1283	1875	92.24%
80	0	0	145.5	145.5	4	0	1283	1431	89.83%

Table 8
The comparison of theoretical energy consumption equipped with fans in long term traffic volume.

vehicle speed km/h	Single-Channel Method				Single Shaft Method				Energy saving ratio
	Number of jet fans		Axial flow fan power	Total Power/(kW)	Number of jet fans		Axial flow fan power	Total Power/(kW)	
	Left Line	Right Line	Single-channel/(kW)		Left Line	Right Line	Single shaft/(kW)		
30	61	57	145.5	4511.5	54	14	1803	4319	−4.45%
40	48	44	145.5	3549.5	42	6	1803	3579	0.82%
50	23	20	145.5	1736.5	26	0	1803	2765	37.20%
60	10	12	145.5	959.5	10	0	1803	2173	55.84%
70	1	2	145.5	256.5	0	0	1803	1803	85.77%
80	0	0	145.5	145.5	0	0	1803	1803	91.93%

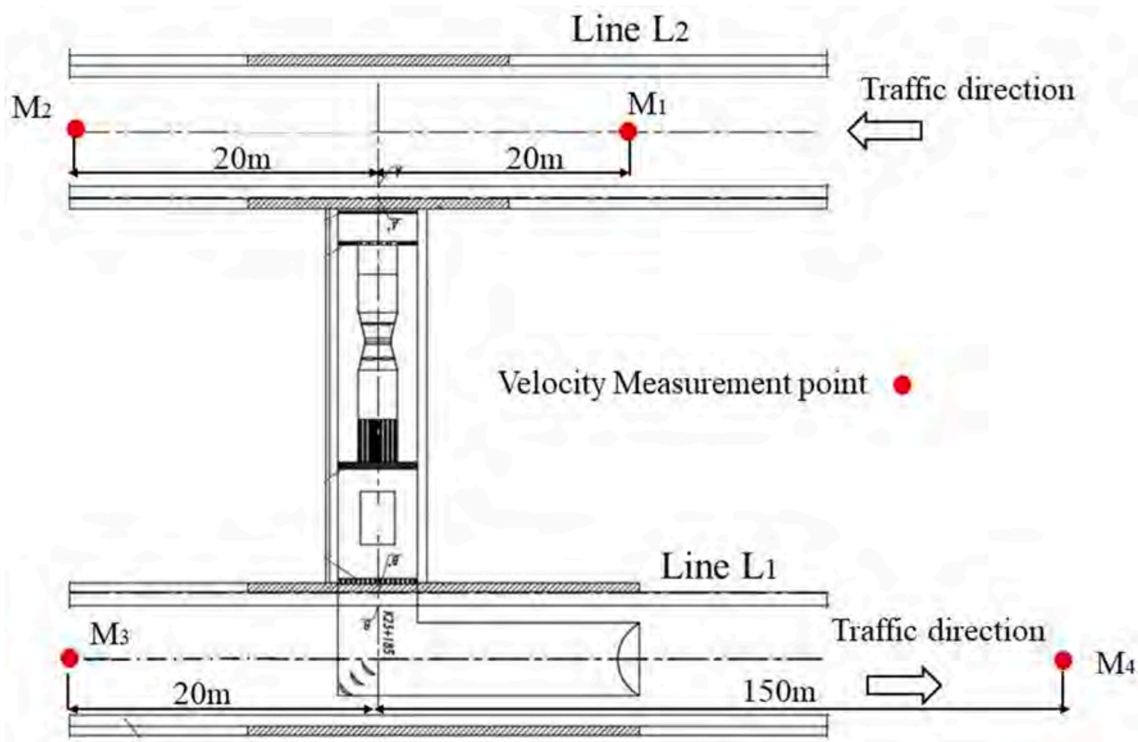

Fig. 21. Wind speed measurement point in the tunnel.

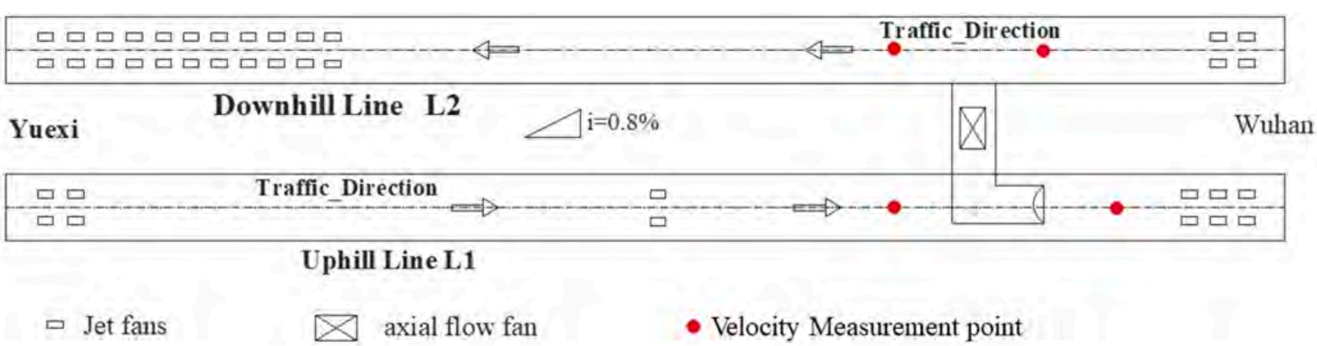

Fig. 22. Ventilation test working condition No.3 of the Mingtang Mountain Tunnel.

Table 9
Field ventilation test program and results of the Mingtang Mountain Tunnel.

	Number of fans		Velocity (m/s)			
No.	Jet fans	axial flow fans	M_1	M_2	M_3	M_4
1	0	0	1.29	1.32	1.36	1.26
2	0	1	2.37	1.44	1.50	2.12
3	38	1	3.51	2.72	1.98	2.70

4.2. Discussion on emergency ventilation and smoke extraction scheme

Fire safety is the core of tunnel disaster prevention (He et al., 2018). Tunnel ventilation systems must be able to support self-evacuation and rescue efforts during emergency incidents (Fan et al., 2018; Tang et al., 2016, 2018). In case of fire in tunnel, in order to effectively discharge smoke. The jet fans located upstream of the fire source should be turned on first so that the directional wind speed to the downstream can be formed in the tunnel. Then start the jet fans located downstream of the fire source to minimize the impact on smoke stability (Hu et al., 2008). The single-channel method adopts the longitudinal smoke extraction, which is effective in one-way traffic condition.

Under normal operation, the axial fan in single-channel combined with jet fans is used for ventilation. In case of fire, according to Bernoulli's Principle, the jet fans make the joint between tunnel and single-channel forms a negative pressure zone. The smoke in the tunnel will enter the adjacent tunnel through the single-channel, which will reduce the smoke extraction efficiency of the ventilation system. Therefore, when the fire occurs in channel L_{11}, channel L_{21} and channel L_{22}, the single channel should be closed first.

4.2.1. The fire occurs in channel L_{11} and channel L_{21}

Keep the jet fans open and the tunnel ventilation direction is the original driving direction. Before evacuation of people located upstream of the fire source, the tunnel ventilation wind speed should be controlled at the critical velocity to hold the tunnel reverse smoke. After the evacuation of upstream people, the direction of the jet fans should be changed to exhaust smoke through the tunnel entrance.

4.2.2. The fire occurs in channel L_{12} and channel L_{22}

Keep the jet fans open and the tunnel ventilation direction is the

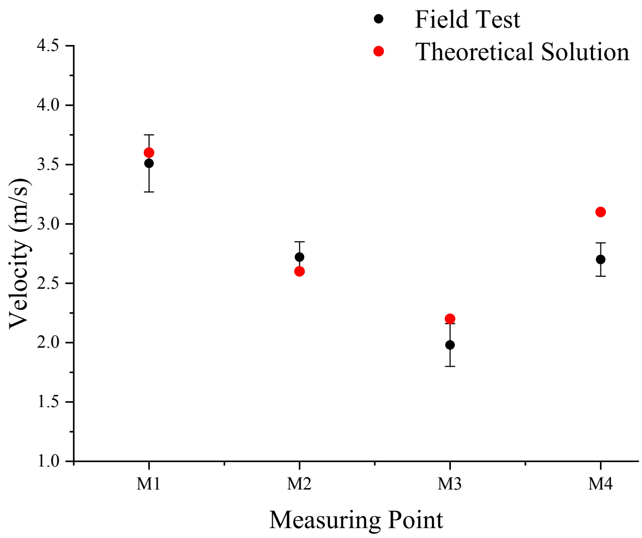

Fig. 23. Results comparison between field test and theoretical solution.

original driving direction. Before evacuation of people located upstream of the fire source, the tunnel ventilation wind speed should be controlled at the critical velocity to hold the tunnel reverse smoke. After the evacuation of upstream people, it is necessary to strengthen the smoke extraction and increase the wind speed in the same direction as before. When the fire occurs in channel L_{12}, the single-channel could be used to supplement air to accelerate the smoke extraction.

4.3. Discussion on limitation of single channel ventilation method

Excessive wind speed in road tunnel will increase the vehicle driving insecurity. As discussed in Section 3.4, the design wind speed of one-way traffic tunnel should be less than 10 m/s, and no more than 12 m/s in special cases, according to Guidelines for Design of Ventilation of Highway Tunnels (Ministry of Communications of PRC, 2014). As a result, the single-channel method cannot be used in ultra-long tunnels alone, especially in the case that the required air volume of the both lines of tunnel are greater than the maximum allowable air supply volume of the tunnel. As calculated in Section 3.3.4 example 6, the applicable scope L_{max} of the tunnel are all less than 12500 m.

It is the further research direction to consider the combined ventilation of single channel and vertical and inclined shaft. The vertical and inclined shaft could effectively discharge the polluted air in the tunnel and send fresh air to reduce the concentration of pollutants in the tunnel and significantly reduce the wind speed in the tunnel. The combination of shafts and single-channel provides a new idea for the ventilation of ultra-long mountains tunnels in the future.

However, the single-channel ventilation is not recommended if the distance between the two lines of tunnel, which is the length of a single channel, is too large or the construction of single-channel is full of difficulty, especially in subsea tunnels.

5. Conclusion

This paper proposes a new longitudinal ventilation method, single channel blowing-in ventilation method, introduces its calculation methodology, analyses six cases, and proves its effectiveness after applying it to the China Mingtang Mountain Tunnel. The optimal location of single-channel x_{fit} enable the total ventilation energy consumption in serving period P_{total} to be the minimal, but usually it cannot let one-year energy consumption P_{one} reach the minimum. The single-channel system shows a better energy-efficient property from a long-term perspective than from a one-year view. For the whole serving period, x_{fit} and P_{total} is relatively fixed when the traffic volume changes linearly.

The main strengths of single channel blowing-in method are: (1) Compared with conventional vertical-shaft ventilation, the single-channel system can achieve a better energy-saving effect and saves the construction costs of shafts. (2) Compared with Double-Hole Complementary Ventilation, it simplifies the ventilation organization of ventilation system in normal condition, and surmounts the limitation that required air volume of two lines should be distinct.

CRediT authorship contribution statement

Chao Guo: Methodology, Writing - original draft, Formal analysis. **Zhiyuan Li:** Writing - review & editing, Formal analysis. **Hehua Zhu:** Conceptualization, Supervision. **Li Zhao:** Methodology. **Zhiguo Yan:** Conceptualization, Methodology, Supervision, Resources, Project administration.

Declaration of Competing Interest

The authors declared that we have no conflicts of interest of this work.

Acknowledgements

The authors would like to acknowledge the financial supports from the Ministry of transport construction technology project MOT (2013318J02120), the major special research project [2018]3011 in Guizhou province and the Taihang Mountian Highway(KT11) research project in Hebei province.

The authors appreciate the support of the Anhui Transportation Holding Group Co., Ltd and the Anhui Transport Consulting & Design Institute Co., Ltd. in demonstration application of Mingtang Mountain Tunnel.

References

Asagami, K., Nagataki, K., 1988. Operation And Adequacy Of The New Ventilation System Of The Kan-Etsu Road Tunnel—Papers Presentes At The 6th International Symposium On The Aerodynamics And Ventilation Of Vehicle Tunnels, DURHAM, 27-29 Sept 1988.

Berner, M. A., Day, J. R., 1991. A New Concept for Ventilation Long Twin-tube Tunnels. In: 7th International Symposium on the Aerodynamics and Ventilation of Vehicle Tunnels, Cranfield UK, pp. 811–820.

Betta, V., Cascetta, F., Musto, M., Rotondo, G., 2009. Numerical study of the optimization of the pitch angle of an alternative jet fan in a longitudinal tunnel ventilation system. Tunn. Undergr. Space Technol. 24 (2), 164–172. https://doi.org/10.1016/j.tust.2008.06.002.

Betta, V., Cascetta, F., Musto, M., Rotondo, G., 2010. Fluid dynamic performances of traditional and alternative jet fans in tunnel longitudinal ventilation systems. Tunn. Undergr. Space Technol. 25 (4), 415–422. https://doi.org/10.1016/j.tust.2010.02.006.

Carvel, R.O., Beard, A.N., Jowitt, P.W., 2001. The influence of longitudinal ventilation systems on fires in tunnels. Tunn. Undergr. Space Technol. 16 (1), 3–21. https://doi.org/10.1016/S0886-7798(01)00025-6.

Chai, L., Wang, X., Han, X., Song, J., Lei, P., Xia, Y., Wang, Y., 2018. Complementary ventilation design method for a highway twin-tunnel based on the compensation concept. Mathe. Probl. Eng. 2018 https://doi.org/10.1155/2018/2393272. Article ID 2393272.

Chan, L.Y., Zeng, L., Qin, Y., Lee, S.C., 1996. CO concentration inside the Cross Harbor Tunnel in Hong Kong. Environ. Int. 22 (4), 405–409. https://doi.org/10.1016/0160-4120(96)00028-1.

Chang, T.Y., Rudy, S.J., 1990. Roadway tunnel air quality models. Environ. Sci. Technol. 24 (5), 672–676.

Chen, Y., Lin, Y., Lu, M., Wang, Y., 2016. A matlab-based traffic prediction system. In: 2016 International Computer Symposium (ICS). IEEE Computer Society, Los Alamitos, CA, USA, pp. 290–293. https://doi.org/10.1109/ICS.2016.0065.

Costantino, A., Musto, M., Rotondo, G., Zullo, A., 2014. Numerical analysis for reduced-scale road tunnel model equipped with axial jet fan ventilation system. Energy Procedia 45, 1146–1154. https://doi.org/10.1016/j.egypro.2014.01.120.

Fan, C., Zhang, L., Jiao, S., Yang, Z., Li, M., Liu, X., 2018. Smoke spread characteristics inside a tunnel with natural ventilation under a strong environmental wind. Tunn. Undergr. Space Technol. 82, 99–110. https://doi.org/10.1016/j.tust.2018.08.004.

Guo, C., Wang, M., Yang, L., Sun, Z., Zhang, Y., Xu, J., 2016. A review of energy consumption and saving in extra-long tunnel operation ventilation in China. Renew. Sustain. Energy Rev. 53, 1558–1569. https://doi.org/10.1016/j.rser.2015.09.094.
Guo, Q.C., Yan, Z.G., Zhu, H.H., Shen, Y., 2013. Numerical simulation on fire characteristics and smoke control of a longitudinal ventilation road tunnel. In: World Conference of Acuus: Advances in Underground Space Development, pp. 232–240.
Guo, Q., Zhu, H., Zhang, Y., Yan, Z., 2020. Theoretical and experimental studies on the fire-induced smoke flow in naturally ventilated tunnels with large cross-sectional vertical shafts. Tunn. Undergr. Sp. Technol. 99, 103359. https://doi.org/10.1016/j.tust.2020.103359.
He, L., Xu, Z., Chen, H., Liu, Q., Wang, Y., Zhou, Y., 2018. Analysis of entrainment phenomenon near mechanical exhaust vent and a prediction model for smoke temperature in tunnel fire. Tunn. Undergr. Space Technol. 80, 143–150. https://doi.org/10.1016/j.tust.2018.06.011.
Hu, L.H., Peng, W., Huo, R., 2008. Critical wind velocity for arresting upwind gas and smoke dispersion induced by near-wall fire in a road tunnel. J. Hazard. Mater. 150, 68–75. https://doi.org/10.1016/j.jhazmat.2007.04.094.
Ministry of Communications of PRC, 2014. Guidelines for Design of Ventilation of Highway Tunnels (JTG/T D70/2-02-2014). China Communications Press, Beijing (in Chinese).
Lesser, N., Horowitz, F., King, K., 1987. Transverse ventilation system of the Holland tunnel evaluated and operated in semitransverse mode. Transp. Res. Rec. 24–28.
Liu, S., Liu, X., Zhang, G., 2011. Numerical analysis of semi-transverse ventilation of extra-long road tunnel. In: 2011 International Conference on Intelligent Computation Technology and Automation (ICICTA). IEEE Computer Society, China, pp. 848–852. https://doi.org/10.1109/ICICTA.2011.220.
Pei, G., Pan, J., 2014. Numerical study on different series modes of jet fan in a longitudinal tunnel ventilation system. Mathe. Probl. Eng., 194125 https://doi.org/10.1155/2014/194125.
PIARC, 2012. Road Tunnels: Vehicle Emissions and Air Demand for Ventilation. World Road Association.
Sun, S., Zhang, C., Yu, G., 2006. A Bayesian network approach to traffic flow forecasting. IEEE Trans. Intell. Transp. Syst. 7 (1), 124–132. https://doi.org/10.1109/TITS.2006.869623.
Tang, F., He, Q., Mei, F., Wang, Q., Zhang, H., 2018. Effect of ceiling centralized mechanical smoke exhaust on the critical velocity that inhibits the reverse flow of thermal plume in a longitudinal ventilated tunnel. Tunn. Undergr. Space Technol. 82, 191–198. https://doi.org/10.1016/j.tust.2018.08.039.
Tang, F., Li, L.J., Mei, F.Z., Dong, M.S., 2016. Thermal smoke back-layering flow length with ceiling extraction at upstream side of fire source in a longitudinal ventilated tunnel. Appl. Therm. Eng. 106, 125–130. https://doi.org/10.1016/j.applthermaleng.2016.05.173.
Vauquelin, O., Wu, Y., 2006. Influence of tunnel width on longitudinal smoke control. Fire Saf. J. 41 (6), 420–426. https://doi.org/10.1016/j.firesaf.2006.02.007.
Wang, M., Tian, Y., Yu, L., Wang, X., Zhang, Z., Yan, G., 2019a. Research on the wind pressure coefficient in natural wind calculations for extra-long highway tunnels with shafts. J. Wind Eng. Ind. Aerodyn. 195, 104020. https://doi.org/10.1016/j.jweia.2019.104020.
Wang, Y.Q., Jiang, X.M., Wu, Y.K., Xie, Y.K., 2015. Analysis on Applicability of twin-tube complementary ventilation in road tunnel. Modern Tunnell. Technol. 52 (3), 14–21 (in Chinese).
Wang, Y.Q., Hu, Y.J., Deng, M., Xia, F.Y., Xie, Y.L., 2014. Complementary ventilation operational test in large longitudinal slope double-hole tunnel. J. Traffic Transport. Eng. 14 (5), 29–35 (in Chinese).
Wang, M., Wang, X., Yu, L., Deng, T., 2019b. Field measurements of the environmental parameter and pollutant dispersion in urban undersea road tunnel. Build. Environ. 149, 100–108. https://doi.org/10.1016/j.buildenv.2018.11.036.
Xia, F.Y., Wang, Y.Q., Jiang, X.M., 2013. Analysis and field test about operation ventilation effect of dabieshan highway tunnel. Appl. Mech. Mater. 438–439, 1000–1003. https://doi.org/10.4028/www.scientific.net/AMM.438-439.1000.
Xia, F.Y., Xie, Y.L., Wang, Y.Q., Hu, Y.J., 2014. Complementary ventilation modes of extra-long highway tunnel. J. Traffic Transport. Eng. 14 (6), 27–34 (in Chinese).
Yamada, N., Ota, Y., 1999. Safety systems for the Trans-Tokyo Bay Highway Tunnel project. Tunn. Undergr. Space Technol. 14 (1), 3–12. https://doi.org/10.1016/S0886-7798(99)00008-5.
Yan, Z.G., Yang, Q.X., Wang, M.N., Zhu, H.H., 2006. Experimental study of shaft ventilation modes for road tunnels in case of fire. China Civil Eng. J. 39 (11), 101–106 (in chinese).
Yan, Z.G., Zhu, H.H., Yang, Q.X., 2006. Large-scaled fire testing for long-sized road tunnel. Tunnell. Underg. Space Technol. Incorporat. Trenchless Technol. Res. 21 (3) https://doi.org/10.1016/j.tust.2005.12.142, 282–282.
Zhang, Y.X., Shen, Y., Carvel, R., Zhu, H.H., Zhang, Y.P., Yan, Z.G., 2020. Experimental investigation on the evacuation performance of pedestrians in a three-lane urban tunnel with natural ventilation in a fire scenario. Tunn. Undergr. Sp. Technol. 103634. https://doi.org/10.1016/j.tust.2020.103634.
Zhang, Y.X., Yan, Z.G., Zhu, H.H., Shen, Y., Guo, Q.H., Guo, Q.C., 2019a. Experimental investigation of pedestrian evacuation using an extra-long steep-slope evacuation path in a high altitude tunnel fire. Sustain. Cities Soc. 46, 101423. https://doi.org/10.1016/j.scs.2019.101423.
Zhang, Z., Zhang, H., Tan, Y., Yang, H., 2018. Natural wind utilization in the vertical shaft of a super-long highway tunnel and its energy saving effect. Build. Environ. 145, 140–152. https://doi.org/10.1016/j.buildenv.2018.08.062.
Zhang, T., Zhang, Y., Xiao, Z.Q., Yang, Z.L., Zhu, H.H., Ju, J.W., Yan, Z.G., 2019b. Development of a novel bio-inspired cement-based composite material to improve the fire resistance of engineering structures. Constr. Build. Mater. 225, 99–111. https://doi.org/10.1016/j.conbuildmat.2019.07.121.
Zhang, T., Zhang, Y., Zhu, H.H., Yan, Z.G., 2021a. Experimental investigation and multi-level modeling of the effective thermal conductivity of hybrid micro-fiber reinforced cementitious composites at elevated temperatures. Compos. Struct. 256, 112988. https://doi.org/10.1016/j.compstruct.2020.112988.
Zhang, Y.X., Zhu, H.H., Guo, Q.H, Carvel, R., Yan, Z.G., 2021b. The effect of technical installations on evacuation performance in urban road tunnel fires. Tunn. Undergr. Sp. Technol. 107, 103608. https://doi.org/10.1016/j.tust.2020.103608.
Zhou, Y., Yang, Y., Mao, Z., Bu, R., Gong, J., Wang, Y., Yi, L., 2019. Analytical and numerical study on natural ventilation performance in single-and gable-slope city tunnels. Sustainable Cities Soc. 45, 258–270. https://doi.org/10.1016/j.scs.2018.11.034.